

Coagulation of aqueous graphene oxides in presence of metal cations

Xiaobin Zhu^{a,b,*}, Bin Zuo^a, Liang Zhang^a, Zhengcun Zhou^a, Lun Yang^{c,*}, Jinlei Zhang^d, Shuyi Wu^d, Sheng Yu^e

^aSchool of Mechano-Electronic Engineering, Suzhou Vocational University, Suzhou, Jiangsu 215104, China, emails: zxbblack@163.com (X.B. Zhu), zuobinjstu@163.com (B. Zuo), 190973176@qq.com (L. Zhang), zzc@jssvc.edu.cn (Z.C. Zhou)

^b3C-Product Intelligent Manufacturing Engineering Technology Research and Development Center of Jiangsu Province, Suzhou, Jiangsu 215104, China

^cInstitute for Advanced Materials, Hubei Key Laboratory of Pollutant Analysis & Reuse Technology, Hubei Normal University, Huangshi 435002, China, email: yanglun@hbnu.edu.cn (L. Yang)

^dJiangsu Key Laboratory of Micro and Nano Heat Fluid Flow Technology and Energy Application, School of Mathematics and Physics, Suzhou University of Science and Technology, Suzhou, Jiangsu 215009, China, emails: zhangjinlei199119@126.com (J.L. Zhang), woaiwuliban@163.com (S.Y. Wu)

^eLaboratory of Environment and Analysis, Suzhou Vocational University, Suzhou, Jiangsu 215104, China, email: yus@jssvc.edu.cn (S. Yu)

Received 6 May 2021; Accepted 26 August 2021

ABSTRACT

With the extensive use of graphene oxide (GO) in research and application, the negative impact of water-soluble graphene oxide on the environment has to be considered. It is significant to find a suitable method to remove GO from water. In this study, sulfates were used as the coagulants for GO removal. The experimental results showed that cations as Mg^{2+} , Al^{3+} , Ca^{2+} , Co^{2+} , Ni^{2+} , Cu^{2+} , Zn^{2+} , Mn^{2+} interacted with GO and GO would agglomerate then. However, low-concentration Na^+ , K^+ and SO_4^{2-} did not show any coagulation capacity. The temperature, equilibrium time and the initial concentration of cations and GO would affect the coagulation capacities. Among the selected sulfates, aluminum sulfate, calcium sulfate and copper sulfate had higher coagulation capacities, which were 4,772; 1,149 and 1,451 mg/g, respectively. In addition, the metallic cations mentioned were easy to obtain, so they were promising coagulants for the elimination of GO from water.

Keywords: Coagulation; Graphene oxide; Metal cations; Adsorption charge neutralization

1. Introduction

Due to their excellent mechanical, electrical, optical and thermal properties, graphene and its derivatives have been widely concerned by researchers in recent years [1–6]. Graphene oxide (GO) is an important derivative of graphene with wider application prospects as it is easy to process and contains abundant functional groups [7–10]. Nevertheless, GO is water-soluble, which means it may influx into the aquatic system in the process of preparation and application.

Researchers have pointed out that GO exhibited potential toxicity in bacteria, animals, plants and human cells [11–14]. Thus GO must be removed from the aquatic environment and appropriate methods are urgently needed.

Photo-induced degradation [15] and coagulation [16–22] were the common methods to remove GO. The capacities of coagulation are more promising than those of photo-degradation because of its less reaction time (usually within an hour) and no additional energy. For instance, Wang et al. [18] reported the GO removal capacities could

* Corresponding authors.

reach 565.8 mg/g on Mg/Al/La-calcined layered double hydroxides (CLDHs) and 558.6 mg/g on Ca/Al/La-CLDHs at GO initial concentration of 120 mg/L and CLDHs content of 0.2 g/L. The removal percentage of GO exceeds 90% within the contact time of 30 min. Yuan et al. [19] found that MgAl-mixed metal oxide (MgAl-MMO) exhibited ultra-high GO adsorption capacity of 984.2 mg/g, which is highest among Al-based oxides/hydroxides. A study by Duan et al. [20] found alum is also a good coagulant whose removal capacity is 960 mg/g. Alum is quite different from Al-based oxides/hydroxides as a coagulant because it is water-soluble and the Al species in the aqueous phase play a major role in coagulation. Ca^{2+} in an aqueous solution can also coagulate GO. For example, cement, mainly composed of calcium salts, has a coagulation capacity of 5,981.2 mg/g which is the highest removal capacity up to now [21].

It can be seen that the above coagulants are mainly composed of aluminum salt or calcium salt, and cations play a major role in the coagulation process [16–21]. However, the existing coagulants usually consist of two or more cations. For example, alum contains K^+ and Al^{3+} . Although Duan et al. [20] attributed the coagulation of graphene oxides to Al species, they have not proved that K^+ was useless. In order to explain the effect of cations in the coagulation of GO, the study of single cations is more effective. Being made relevant attempts [22], the dosages of coagulants were far greater than those of GO in their experiments. Taking Cu^{2+} as an example, the dosage of coagulant was 134.45 mg, 90 times that of GO, which was not conducive to show the coagulation ability of metal cations. We have reduced the quality of coagulants to twice or less than that of GO. The effects of cations dosage, GO concentration, contact time, and temperature on GO coagulation behavior were investigated. The results will be of great significance to the development of new coagulants for GO and also contribute to the synthesis of GO composites.

2. Experimental section

2.1. Materials

The GO sheets (ID XF002-1, planar size: 0.5–5 μm) were purchased from Jiangsu Xfnano Materials Tech Co., Ltd., (Nanjing, China). Sulfates (Na_2SO_4 , $\text{MgSO}_4 \cdot 7\text{H}_2\text{O}$, $\text{Al}_2(\text{SO}_4)_3 \cdot 18\text{H}_2\text{O}$, K_2SO_4 , $\text{CaSO}_4 \cdot 2\text{H}_2\text{O}$, $\text{CoSO}_4 \cdot 7\text{H}_2\text{O}$, $\text{NiSO}_4 \cdot 6\text{H}_2\text{O}$, $\text{ZnSO}_4 \cdot 7\text{H}_2\text{O}$, $\text{CuSO}_4 \cdot 5\text{H}_2\text{O}$, $\text{MnSO}_4 \cdot \text{H}_2\text{O}$), NaCl and Na_2CO_3 were obtained from Sinopharm Chemical Reagent Co., Ltd., (China) and used to provide cations. The sulfates were all analytical grades. All the chemicals were used as received without further purification. Deionized (DI) water was used in all the experiments.

2.2. Preparation of GO suspension

GO suspension was prepared by intermittent ultrasonic method to prevent chemical reaction at high temperature. 100 mg GO sheets were added to a beaker containing about 150 mL DI water and then the mixture was ultrasonically treated. After every 15 min, the ultrasound was stopped for 30 min and then continued. After the ultrasound time reached 8 h (excluding the time when the ultrasound stops),

the suspension was allowed to stand for 1 h to cool down to room temperature and then diluted to 200 mL. The pH of the initial GO solution was 3.5.

2.3. Coagulation experiments

All the experiments were carried out at 25°C (except the experiments for different coagulation temperatures), and a double beam UV/Vis spectrophotometer (Rayleigh UV2601, China) was used to analyze the concentration of GO. To initiate each test, GO suspension with different concentrations and the sulfate solution were mixed together in a vial to obtain a 10 mL mixture. The initial GO concentration (C_{GO0}) in the mixture was 50, 100, 200 or 400 mg/L. The mixture was stirred for 1 h and then equilibrated for 2 h to settle the flocs. Photographs were taken by a Canon digital single-lens reflex (DSLR) camera immediately after the reaction. About 4 mL supernatant was then withdrawn and diluted x ($x = C_{\text{GO0}}/50$) times. The ultraviolet-visible (UV-Vis) absorption spectrum of GO after dilution was measured and the equilibrium concentration of GO (C_{GOe}) could be calculated. Experiments at other temperatures (40°C, 55°C or 70°C) underwent a similar process, except that an extra half-hour cooling process was added at the end of each experiment to make the mixture return to normal temperature and become stable. The coagulation capacity (q_e) for GO and the removal percentage (R), were calculated using the following equations:

$$q_e = \frac{C_{\text{GO0}} - C_{\text{GOe}}}{C_s} \quad (1)$$

$$R = \frac{C_0 - C_e}{C_0} \times 100\% \quad (2)$$

where C_s was the initial concentration of the sulfate. Note that the qualities of crystallized water in sulfates were not considered in order to make the comparison between sulfates more accurate.

2.4. Characterization of the coagulation products

100 mL mixture of GO and sulfate (aluminum sulfate, calcium sulfate or cupric sulfate) with initial concentrations of 400 and 800 mg/L was stirred for 1 h and then equilibrated for 2 h. The mixture was centrifuged at 6,000 rpm for 5 min and the precipitate was dried at 70°C for 24 h. The products with aluminum ions, calcium ions and copper ions added were labeled as GO-Al, GO-Ca and GO-Cu respectively. Scanning electron microscopy (SEM) images were performed on the Zeiss GeminiSEM 300 (Germany) scanning electron microscope and the FEI Quanta 450 FEG scanning electron microscope. Powder X-ray diffraction (XRD) patterns were recorded on the Bruker D8 ADVANCE (Germany) XRD instrument using Cu K_α radiation, and the Fourier-transform infrared (FTIR) spectra were obtained using the KBr Pellet Method on the Thermo Fisher Nicolet (USA) spectrometer. Zeta potential was determined using a Malvern Zetasizer Nano ZS90 (US) zeta potential meter.

3. Results and discussion

In order to eliminate the influence of anion on the experiment, we tested the coagulation of GO in the presence of excess anion. As shown in Fig. S1, flocs occurred when the dosage of NaCl was 50 times as much as that of GO. When the same amount of sodium sulfate or carbonate was added into GO suspension, no precipitate was observed. It could be seen that anions affected coagulation, and the effect of chloride ion was greater than that of sulfate ion or carbonate ion. In addition, many metallic carbonates are insoluble in water, so sulfates were employed in our experiments.

The concentration of GO was usually confirmed by the UV-Vis spectrophotometry at the maximum absorption wavelength which was about 227 nm [23]. However, cations from the sulfates, especially Cu^{2+} ion, showed some absorption at this wavelength (Fig. S2a). The absorbance of 200 mg/L CuSO_4 is as high as 0.554, which will inevitably affect the measurement of the GO concentration. Therefore, it is not feasible to determine the GO concentration by measuring the absorbance at 227 nm in our experiments. After the UV-Vis absorption spectra were zoomed-in (Fig. S2b), it was found that the absorbance of all the cations at 336 nm was very small (no more than 0.002). The UV-Vis spectra of GO with different concentrations are presented in Fig. S3a and it was found that the adsorption intensity of aqueous GO solution at 336 nm obeys Beer–Lambert Law at GO concentration below 50 mg/L (Fig. S3b). The absorption coefficient (α) for GO at this wavelength was 11.58 L/(g cm). So the concentration of GO was determined by measuring the absorbance at 336 nm in this work.

Fig. 1 shows the results of the coagulation experiment when the initial GO concentration (C_{GO}) was 100 mg/L and the equilibrium time was 2 h. The corresponding initial sulfate concentrations (C_s) ranged from 40 to 200 mg/L (2.5–200 mg/L for aluminum sulfate). It can be found from the spectra that Na^+ , Mg^{2+} , K^+ , Ca^{2+} , Co^{2+} , Ni^{2+} , Zn^{2+} and Mn^{2+} could not coagulate GO under such experimental

conditions. No flocs could be seen in the corresponding photographs (Fig. S4), which also indicates that GO was not coagulated. GO was not coagulated when the concentration of copper ion was less than 80 mg/L (Fig. 1c). When C_s reached 120 mg/L, some of the GO was removed, and the removal rate of GO increased with the increase of C_s . When C_s is 120 mg/L, the coagulation capacity reaches the maximum value of 0.63 g/g (Fig. 1b). When Al^{3+} was added into the GO solution, the coagulation of GO occurred and flocs could be observed even if C_s was only 10 mg/L (Fig. 1d). Most of GO would be removed when the initial concentration reached 20 mg/L, and the coagulation capacity was as high as 4.77 g/g. When the equilibrium time increased to 1 d, GO was also coagulated when the cations were Ca^{2+} , Co^{2+} , Ni^{2+} , Zn^{2+} and Mn^{2+} (Fig. 2). The coagulation capacities of these cations were not much worse than that of Al^{3+} or Cu^{2+} when the initial sulfate concentrations were 200 mg/L. Therefore, cations as Ca^{2+} , Co^{2+} , Ni^{2+} , Zn^{2+} and Mn^{2+} can also be used as coagulants for GO, but their coagulation rate is relatively slow. Contrarily, Na^+ , Mg^{2+} , K^+ did not show any coagulation capacities under the same experimental conditions.

Temperature can affect coagulation [17,18], so variable temperature coagulation experiments have also been carried out (Fig. 3). In these experiments, GO was equilibrated at different temperatures (40°C, 55°C or 70°C) for 2 h and then cooled at 25°C for 0.5 h. The reference samples without cations also experienced the same experimental process. It could be seen that the absorbance of GO at 336 nm increased with the increase of temperature, which indicated that chemical reactions, such as reduction, occurred when GO was heated. Therefore, the relationship between the absorbance and the concentration would change with temperature, and we only analyzed the absorbance of GO without calculating the removal rate or the coagulation capacity. When Na^+ , Mg^{2+} or K^+ was added, the relationship between the absorbance and the temperature was the same as that of the reference sample, which indicated that they did not

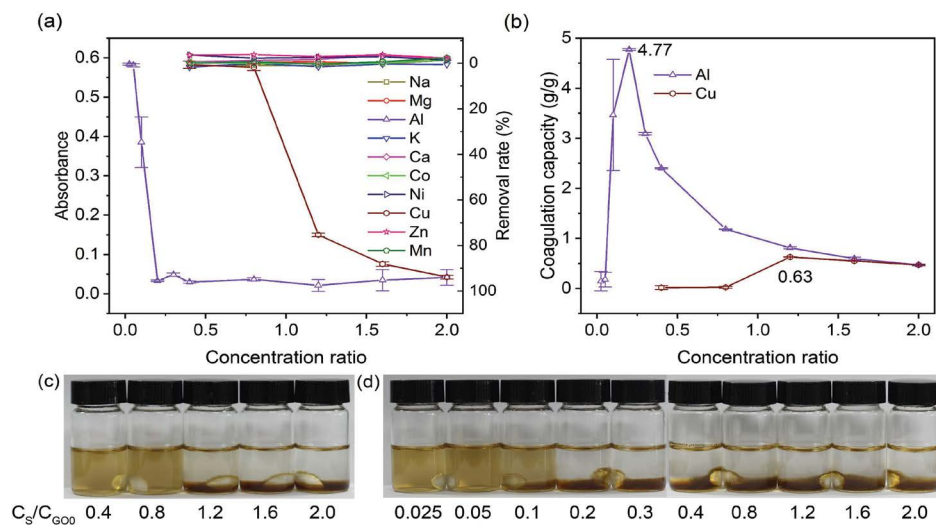


Fig. 1. Coagulation experiments with an initial GO concentration of 100 mg/L. The equilibrium temperature and time were 25°C and 2 h. (a) The absorbance and the removal rates of GO and (b) the coagulation capacities after the coagulation experiments. Digital photographs were taken after equilibrium with (c) Cu^{2+} and (d) Al^{3+} added into the GO suspension.

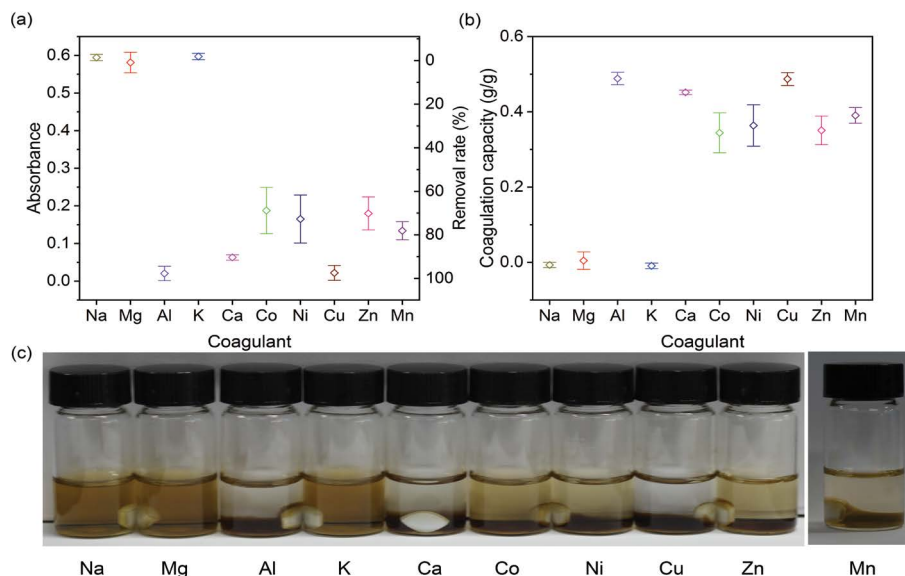


Fig. 2. Coagulation experiments with equilibrium time increase to 1 d ($C_s/C_{GO0} = 2.0$). (a) The absorbance and the removal rates of GO, (b) the coagulation capacities and (c) the digital photographs after the coagulation experiments.

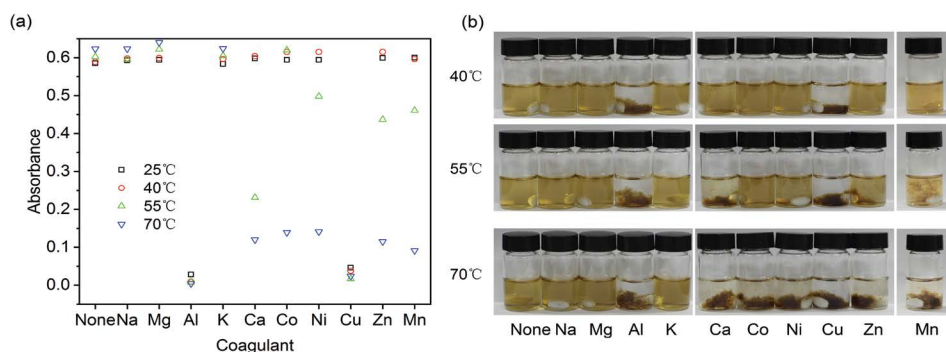


Fig. 3. Coagulation experiments with different equilibrium temperature ($C_s/C_{GO0} = 2.0$). (a) The absorbance of GO and (b) the digital photographs after the coagulation experiments.

have coagulation capacity at high temperature. When Al^{3+} or Cu^{2+} was added, the equilibrium absorbance decreased with the increase of temperature, which meant that coagulation was accelerated under higher temperature. For some other cations such as Ca^{2+} , Co^{2+} , Ni^{2+} , Zn^{2+} or Mn^{2+} , there seemed to be a start-up temperature for coagulation, and the coagulation phenomenon would be obvious when the equilibrium temperature was higher than the start-up temperature. The start-up temperature of Ca^{2+} , Ni^{2+} , Zn^{2+} , Mn^{2+} was about $55^{\circ}C$, while that of Co^{2+} was about $70^{\circ}C$.

The initial GO concentration may also affect coagulation [17,18,21]. As shown in Fig. 4, the removal of GO was studied with other GO initial concentrations of 50, 200 and 400 mg/L. And the initial concentration ratio of the sulfate and GO (C_s/C_{GO0}) ranged from 0.4 to 2.0 for the coagulation experiments. The removal rate of GO by cations other than Al^{3+} and Cu^{2+} was low at an initial GO concentration of less than 50 mg/L. Cu^{2+} showed a coagulation capacity of 0.26 g/g only when the concentration ratio reached 2 (Fig. 4b). For Al^{3+} , however, the removal rate reached 93.2% and the

coagulation capacity was up to 2.33 g/g when the concentration ratio was 0.4. These experimental results were similar to those at the initial GO concentration of 100 mg/L. When the initial GO concentration increased to 200 mg/L, coagulation could be observed in the GO solution with 400 mg/L Mg, Al, Ca, Co, Ni, Cu, Zn or Mn sulfate added (Figs. S5a–d). The removal rates were 73.3%, 100%, 94.8%, 84.5%, 79.0%, 99.7%, 81.4%, 84.1% (Fig. 4c) and the coagulation capacities were 0.366, 0.50, 0.474, 0.422, 0.395, 0.498, 0.407, 0.421 g/g, respectively (Fig. 4d). The order of the coagulation capacities was as follows: $Al^{3+} > Cu^{2+} > Ca^{2+} > Co^{2+} > Mn^{2+} > Zn^{2+} > Ni^{2+} > Mg^{2+}$. Another notable phenomenon was that at this initial GO concentration, the settling speed of the flocs was relatively slow except for the GO solution with aluminum ions. When the initial GO concentration increased to 400 mg/L, the removal rates were no less than 98% and the corresponding coagulation capacity was not less than 0.49 g/g at an initial concentration ratio of 2.0 excepted for Na^{+} or K^{+} (Fig. 4e). It could also be seen from the optical photos that the flocs had settled and the supernatant became

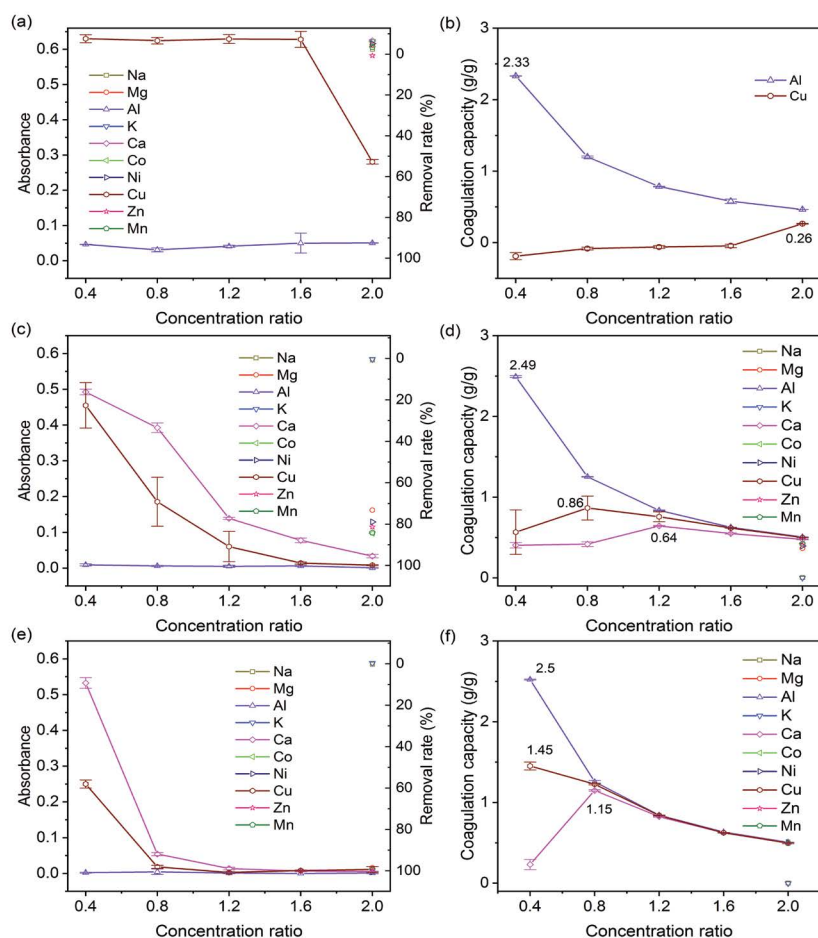


Fig. 4. Coagulation experiments with initial GO concentration of (a and b) 50 mg/L, (c and d) 200 mg/L and (e and f) 400 mg/L. (a,c,e) were the absorbance and the removal rates of GO and (b,d,f) were the coagulation capacities after equilibrium.

transparent (Figs. S5e–h). At this initial GO concentration, the maximum coagulation capacities of Al^{3+} , Ca^{2+} and Cu^{2+} were 2.5, 1.16 and 1.42 g/g, respectively (Fig. 4f). However, sodium sulfate and potassium sulfate did not seem to be able to coagulate GO when C_{GO0}/C_s was no more than 2.0.

According to all the coagulation experiments we had done, the maximum coagulation capacities of aluminum sulfate, calcium sulfate and copper sulfate were 4,772; 1,149 and 1,451 mg/g respectively. The coagulation capacities of other coagulants proposed are listed in Table 1 [16–21,23]. It could be seen that the coagulation capacities of the three sulfates were higher than most of the existing coagulants. Moreover, the coagulation capacity of aluminum sulfate was close to the existing maximum coagulation capacity of 5,981.2 mg/g. At the same time, sulfates are common chemical reagents, which means that their cost is relatively low, so sulfates as coagulants are very promising.

Electric double-layer compression, adsorption charge neutralization, inter-colloid bridging and sediment netting/sweep coagulation were the main mechanisms to illustrate the aggregation of colloid by coagulants [24]. Several characterizations were performed to explore the possible coagulation mechanism. As shown in Figs. 5a and 5b, GO-Al was crumpled which was similar to the morphology of GO [7–10]. No obvious clusters were found on the surface of

Table 1
Comparisons of the coagulation capacity of GO with different coagulants

Coagulants	Removal capacity (mg/g)	References
Mg/Al layered double hydroxide	79.9	16
Ca/Al layered double hydroxide	123	16
Calcined glycerinum-modified Mg/Al layered double hydroxides	448.3	17
Ca/Al/La-CLDHs	558.6	18
Mg/Al/La-CLDHs	565.8	18
MgAl-MMO	984.2	19
Alum	960	20
Cement	5,981.2	21
MB	2,268	23
$\text{Al}_2(\text{SO}_4)_3$	4,772	This study
CaSO_4	1,149	This study
CuSO_4	1,451	This study

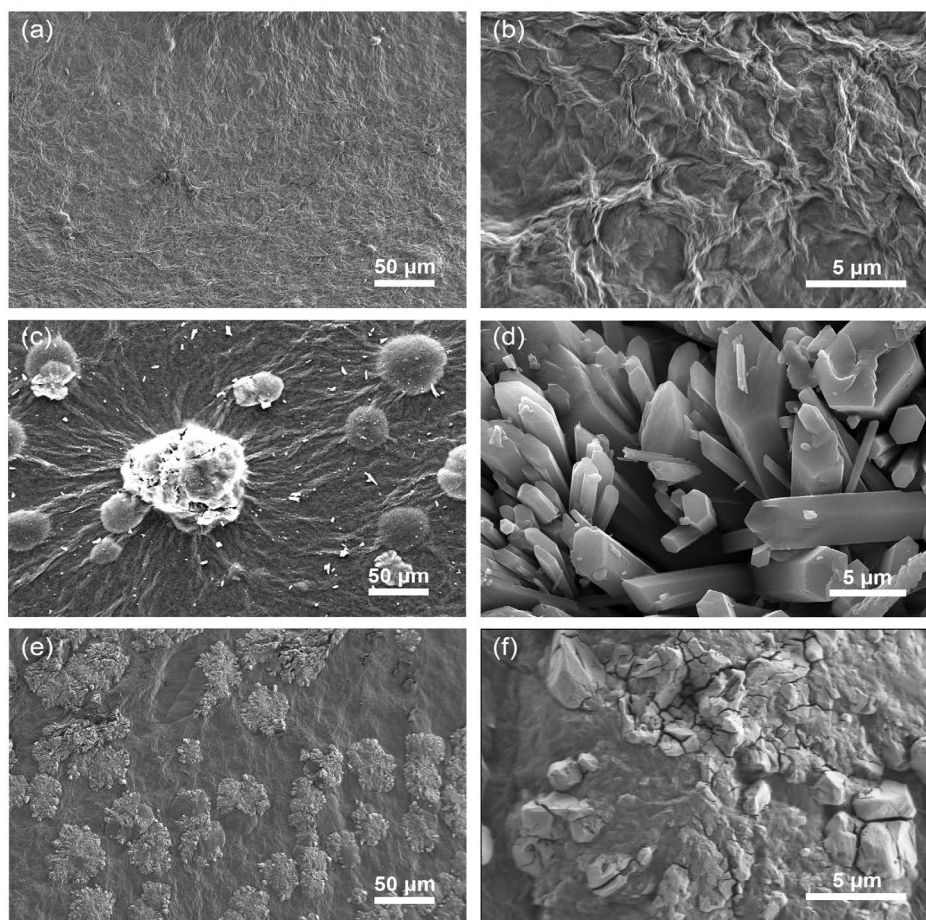


Fig. 5. SEM images of (a) GO-Al at low magnification, (b) GO-Al at high magnification, (c) GO-Ca, (d) clusters in GO-Ca, (e) GO-Cu and (f) clusters in GO-Cu.

GO-Al. On the contrary, when Ca^{2+} and Cu^{2+} were added, clusters were formed on the surface as well as in the interlayer of GO (Figs. 5c–f). The XRD pattern of GO-Al was similar to that of the untreated GO sheets (Fig. S6). Only a sharp peak at 10.4° and a broad peak at 20.8° could be observed in the XRD pattern of GO-Al which were typical peaks of GO [25]. The characteristic peaks of calcium sulfate and copper sulfate appeared in the XRD patterns of GO-Ca and GO-Cu. Therefore, the clusters in the SEM images were the sulfate of copper or calcium. There are no characteristic peaks of other colloids or precipitates (such as copper hydroxide or calcium hydroxide) in the XRD diagrams, so neither inter-colloid bridging nor sediment netting/sweep coagulation was the coagulation mechanism. The zeta potential of GO without adding any coagulant was -35.6 mV (Fig. S7). When Na_2SO_4 was added, the change of zeta potential was small. Even if the amount of Na_2SO_4 was twice that of GO, the absolute value of zeta potential was still as high as 26.1 mV. When it came to CuSO_4 , the value of zeta potential changed greatly. The absolute value of zeta potential was -12.1 mV with 40 mg/L CuSO_4 added. After the addition of Na_2SO_4 and CuSO_4 , the ion concentration in the GO solution was almost the same, but the change of the zeta potential by CuSO_4 was much greater than that of Na_2SO_4 . Therefore, the adsorption charge

neutralization rather than electric double-layer compression was the main coagulation mechanism. FTIR spectra (Fig. S8) of GO showed C=O ($1,717$ cm^{-1}), aromatic C=C ($1,620$ cm^{-1}), C–OH ($1,374$ cm^{-1}), epoxy C–O–C ($1,223$ cm^{-1}), and alkoxy C–O ($1,044$ cm^{-1}) stretching vibrations [26–28]. The peaks at $1,223$ and $1,717$ cm^{-1} of the samples after coagulation were obviously weakened, which meant that C=O and C–O–C interacted with the metal ions during coagulation.

4. Conclusion

In this work, the coagulation behaviors of GO in presence of the metal cations were investigated through a series of coagulation experiments. The experimental results showed that Mg^{2+} , Al^{3+} , Ca^{2+} , Co^{2+} , Ni^{2+} , Cu^{2+} , Zn^{2+} or Mn^{2+} cations could be used as coagulants for GO. The removal capacities were also dependent on the temperature, equilibrium time and the initial concentration of cations and GO. The maximum coagulation capacities of $\text{Al}_2(\text{SO}_4)_3$, CaSO_4 and CuSO_4 were 4.77 , 1.15 and 1.45 g/g, respectively, and the main mechanisms of GO removal by metal cations were adsorption charge neutralization. In addition, the metal cations mentioned were easy to obtain, so they were promising coagulants for the elimination of GO from water.

Supporting information

Fig. S1: The influence of the anions on coagulation. Fig. S2: UV-Vis absorption spectra of the sulfates. Fig. S3: UV-Vis absorption spectra of GO suspension and the correlation between GO concentrations and the absorbance at 336 nm. Fig. S4: Digital photographs taken with the initial GO concentration of 100 mg/L. Fig. S5: Digital photographs taken with the initial GO concentration of 200 and 400 mg/L. Fig. S6: XRD patterns of GO, GO-Al, GO-Ca and GO-Cu. Fig. S7: Zeta potential of GO suspension with different coagulants added. Fig. S8: FTIR spectra of GO, GO-Al, GO-Ca and GO-Cu.

Notes

The authors declare no competing financial interest.

Acknowledgments

This work was supported by the National Natural Science Foundation of China (51801059), Suzhou Municipal Science and Technology Bureau (SS201817, SNG2020055, SYG201939) and the Research Foundation of Suzhou Vocational University (SVU2018YY08). Partial support was also from the Natural Science Foundation of the Jiangsu Higher Education Institutions of China (19KJD470005).

References

- [1] Y. Cao, V. Fatemi, S. Fang, K. Watanabe, T. Taniguchi, E. Kaxiras, P. Jarillo-Herrero, Unconventional superconductivity in magic-angle graphene superlattices, *Nature*, 556 (2018) 43–50.
- [2] D. Xu, B. Cheng, W. Wang, C. Jiang, J. Yu, Ag₂CrO₄/g-C₃N₄/graphene oxide ternary nanocomposite Z-scheme photocatalyst with enhanced CO₂ reduction activity, *Appl. Catal., B*, 231 (2018) 368–380.
- [3] X.M. Yu, P. Han, Z.X. Wei, L.S. Huang, Z.X. Gu, S.J. Peng, J.M. Ma, G.F. Zheng, Boron-doped graphene for electrocatalytic N₂ reduction, *Joule*, 2 (2018) 1610–1622.
- [4] J.R. He, G. Hartmann, M. Lee, G.S. Hwang, Y.F. Chen, A. Manthiram, Freestanding 1T MoS₂/graphene heterostructures as a highly efficient electrocatalyst for lithium polysulfides in Li-S batteries, *Energy Environ. Sci.*, 12 (2019) 344–350.
- [5] J.L. Liu, Y.Q. Zhang, L. Zhang, F.X. Xie, A. Vasileff, S.Z. Qiao, Graphitic carbon nitride-derived N-rich graphene with tuneable interlayer distance as a high-rate anode for sodium-ion batteries, *Adv. Mater.*, 31 (2019) 1901261, doi: 10.1002/adma.201901261.
- [6] J.W. McIver, B. Schulte, F.-U. Stein, T. Matsuyama, G. Jotzu, G. Meier, A. Cavalleri, Light-induced anomalous hall effect in graphene, *Nat. Phys.*, 16 (2020) 38–41.
- [7] R.B. Zhao, C.W. Liu, X.X. Zhang, X.J. Zhu, P.P. Wei, L. Ji, Y.B. Guo, S.Y. Gao, Y.L. Luo, Z.M. Wang, X.P. Sun, An ultrasmall Ru₂P nanoparticles-reduced graphene oxide hybrid: an efficient electrocatalyst for NH₃ synthesis under ambient conditions, *J. Mater. Chem. A*, 8 (2020) 77–81.
- [8] X.B. Zhu, Y. Shan, S.J. Xiong, J.C. Shen, X.L. Wu, Brianyoungite/graphene oxide coordination composites for high-performance Cu²⁺ adsorption and tunable deep-red photoluminescence, *ACS Appl. Mater. Interfaces*, 8 (2016) 15848–15854.
- [9] Y.N. Ma, Y. Yue, H. Zhang, F. Cheng, W.Q. Zhao, J.Y. Rao, S.J. Luo, J. Wang, X.L. Jiang, Z.T. Liu, N.S. Liu, Y.H. Gao, 3D synergistical MXene/reduced graphene oxide aerogel for a piezoresistive sensor, *ACS Nano*, 12 (2018) 3209–3216.
- [10] H.J. Yan, Y. Xie, Y.Q. Jiao, A.P. Wu, C.G. Tian, X.M. Zhang, L. Wang, H.G. Fu, Holey reduced graphene oxide coupled with an Mo₂N-Mo₂C heterojunction for efficient hydrogen evolution, *Adv. Mater.*, 30 (2018) 1704156, doi: 10.1002/adma.201704156.
- [11] J. Zhao, X.S. Cao, Z.Y. Wang, Y.H. Dai, B.S. Xing, Mechanistic understanding toward the toxicity of graphene-family materials to freshwater algae, *Water Res.*, 111 (2017) 18–27.
- [12] O. Akhavan, E. Ghaderi, Toxicity of graphene and graphene oxide nanowalls against bacteria, *ACS Nano*, 4 (2010) 5731–5736.
- [13] X.H. Lv, Y. Yang, Y. Tao, Y.L. Jiang, B.Y. Chen, X.S. Zhu, Z.H. Cai, B. Li, A mechanism study on toxicity of graphene oxide to daphnia magna: direct link between bioaccumulation and oxidative stress, *Environ. Pollut.*, 234 (2018) 953–959.
- [14] M.Y. Wang, Y.X. Sun, X.Y. Cao, G.T. Peng, I. Javed, A. Kakinen, T.P. Davis, S.J. Lin, J.Q. Liu, F. Ding, P.C. Ke, Graphene quantum dots against human IAPP aggregation and toxicity in vivo, *Nanoscale*, 10 (2018) 19995–20006.
- [15] X.Y. Yuan, D. Peng, Q.Y. Jing, J.W. Niu, X. Cheng, Z.J. Feng, W. Wu, Green and effective removal of aqueous graphene oxide under UV-light irradiation, *Nanomaterials*, 8 (2018) 654, doi: 10.3390/nano8090654.
- [16] J. Wang, X. Wang, L. Tan, Y. Chen, T. Hayat, J. Hu, A. Alsaedi, B. Ahmad, W. Guo, X. Wang, Performances and mechanisms of Mg/Al and Ca/Al layered double hydroxides for graphene oxide removal from aqueous solution, *Chem. Eng. J.*, 297 (2016) 106–115.
- [17] Y. Zou, X. Wang, Z. Chen, W. Yao, Y. Ai, Y. Liu, T. Hayat, A. Alsaedi, N.S. Alharbi, X. Wang, Superior coagulation of graphene oxides on nanoscale layered double hydroxides and layered double oxides, *Environ. Pollut.*, 219 (2016) 107–117.
- [18] J. Wang, Y. Li, W. Chen, J. Peng, J. Hu, Z. Chen, T. Wen, S. Lu, Y. Chen, T. Hayat, B. Ahmad, X. Wang, The rapid coagulation of graphene oxide on La-doped layered double hydroxides, *Chem. Eng. J.*, 309 (2017) 445–453.
- [19] X. Yuan, J. Niu, Y. Lv, Q. Jing, L. Li, Ultrahigh-capacity and fast-rate removal of graphene oxide by calcined MgAl layered double hydroxide, *Appl. Clay Sci.*, 156 (2018) 61–68.
- [20] L. Duan, R.J. Hao, Z. Xu, X.Z. He, A.S. Adeleye, Y. Li, Removal of graphene oxide nanomaterials from aqueous media via coagulation: effects of water chemistry and natural organic matter, *Chemosphere*, 168 (2017) 1051–1057.
- [21] X.Y. Yuan, J.W. Niu, J.J. Zeng, Q.Y. Jing, Cement-induced coagulation of aqueous graphene oxide with ultrahigh capacity and high rate behavior, *Nanomaterials*, 8 (2018) 574, doi: 10.3390/nano8080574.
- [22] X. Wen, X. Jin, F. Wang, Y. You, Y. Chu, P.B. Zetterlund, R.K. Joshi, Cation-induced coagulation in graphene oxide suspensions, *Mater. Today Chem.*, 13 (2019) 139–146.
- [23] X.B. Zhu, J.L. Zhang, S.Y. Wu, Z.C. Zhou, Efficient coagulation and removal of aqueous graphene oxide by different dyes, *Desal. Water Treat.*, 217 (2021) 339–349.
- [24] X.B. Zhu, L. Zhang, B. Zuo, Z.C. Zhou, Y.F. Yang, J.L. Zhang, S.Y. Wu, Ion-induced coagulation of hexagonal boron nitride nanosheets in aqueous environment, *Colloid Interface Sci. Commun.*, 44 (2021) 100475, doi: 10.1016/j.colcom.2021.100475.
- [25] S. Liu, J. Tian, L. Wang, H. Li, Y. Zhang, X. Sun, Stable aqueous dispersion of graphene nanosheets: noncovalent functionalization by a polymeric reducing agent and their subsequent decoration with Ag nanoparticles for enzymeless hydrogen peroxide detection, *Macromolecules*, 43 (2010) 10078–10083.
- [26] V. Chandra, J. Park, Y. Chun, J.W. Lee, I.C. Hwang, K.S. Kim, Water-dispersible magnetite-reduced graphene oxide composites for arsenic removal, *ACS Nano*, 4 (2010) 3979–3986.
- [27] C.C. Ding, W.C. Cheng, X.X. Wang, Z.Y. Wu, Y.B. Sun, C.L. Chen, X.K. Wang, S.H. Yu, Competitive sorption of Pb(II), Cu(II) and Ni(II) on carbonaceous nanofibers: a spectroscopic and modeling approach, *J. Hazard. Mater.*, 313 (2016) 253–261.
- [28] Y. Si, E.T. Samulski, Synthesis of water soluble graphene, *Nano Lett.*, 8 (2008) 1679–1682.

Supporting information

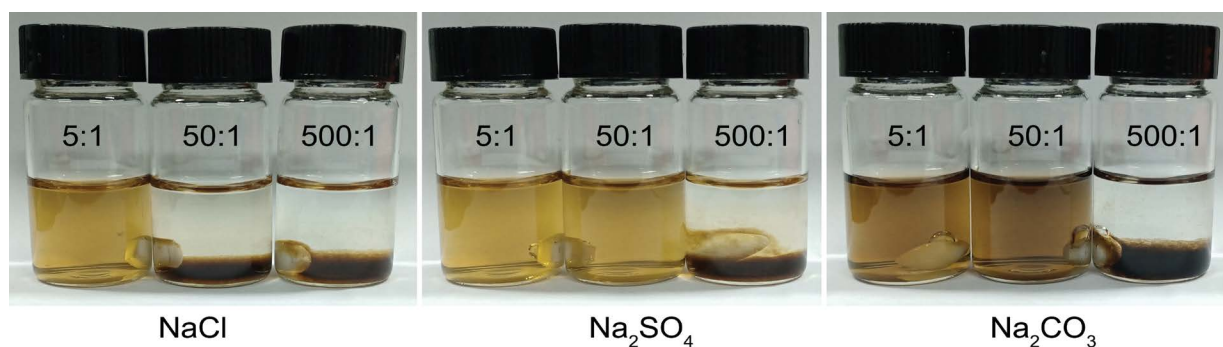


Fig. S1. The influence of the anions to coagulation. The label in the figure is the mass ratio of the sodium salt to GO in the solution. $C_{GO} = 100 \text{ mg/L}$.

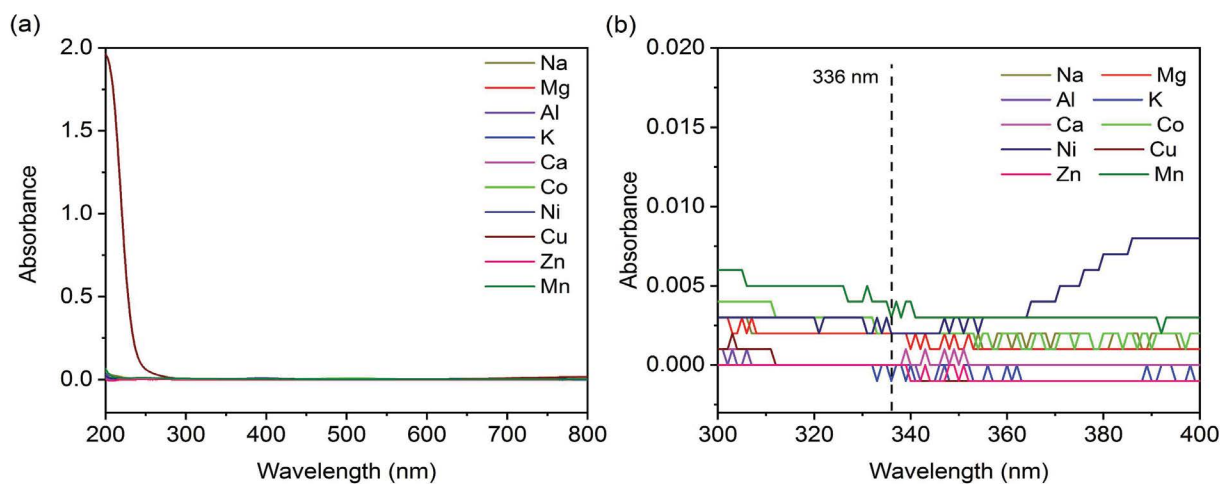


Fig. S2. UV-Vis absorption spectra of the sulfates.

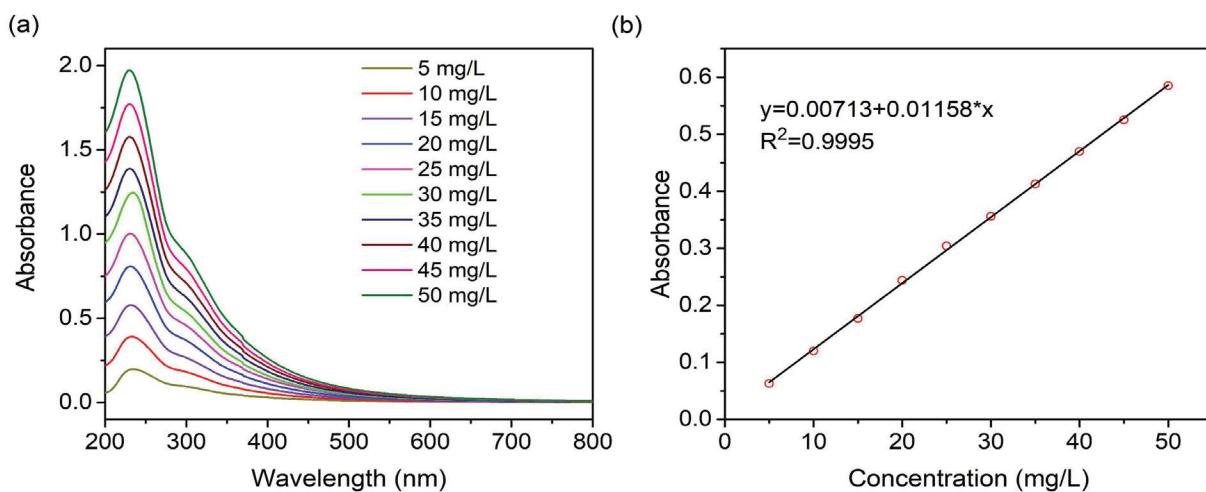


Fig. S3. (a) UV-Vis absorption spectra of GO suspension with different concentrations. (b) The correlation between GO concentrations and its UV absorbance intensity at 336 nm.

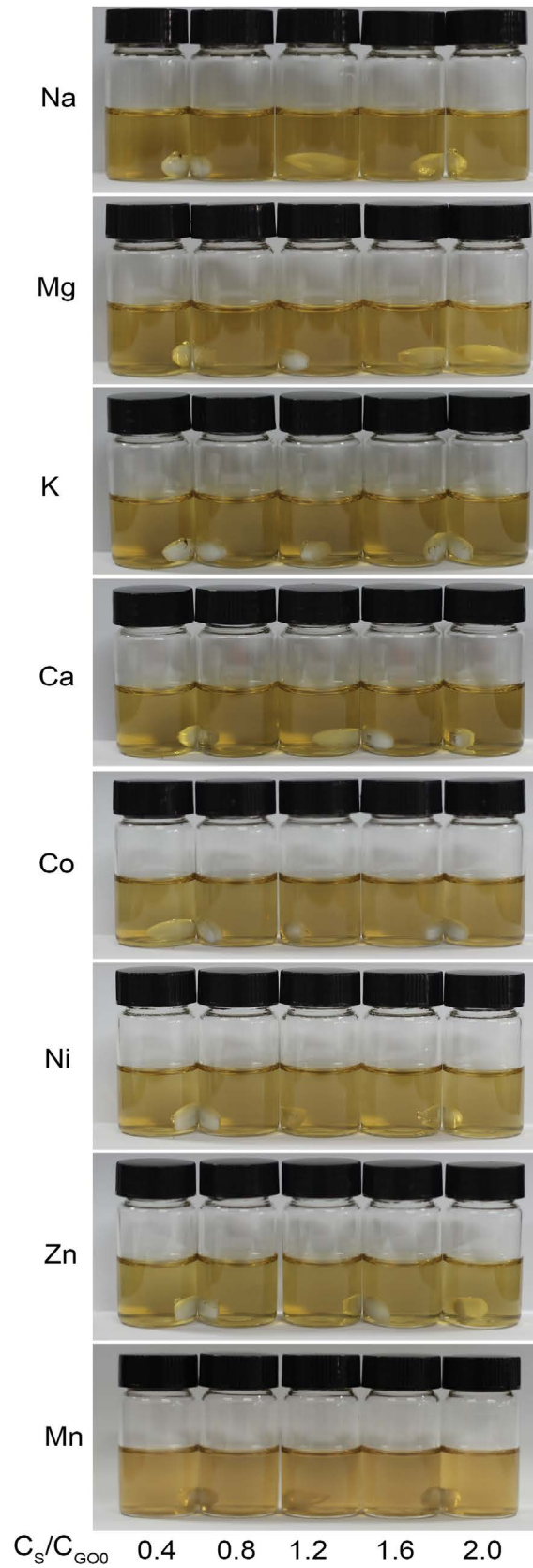


Fig. S4. Digital photographs were taken after equilibrium for 2 h at 25°C with Na^+ , Mg^{2+} , K^+ , Ca^{2+} , Co^{2+} , Ni^{2+} , Zn^{2+} , Mn^{2+} were added into the GO suspension. The initial GO concentration was 100 mg/L.

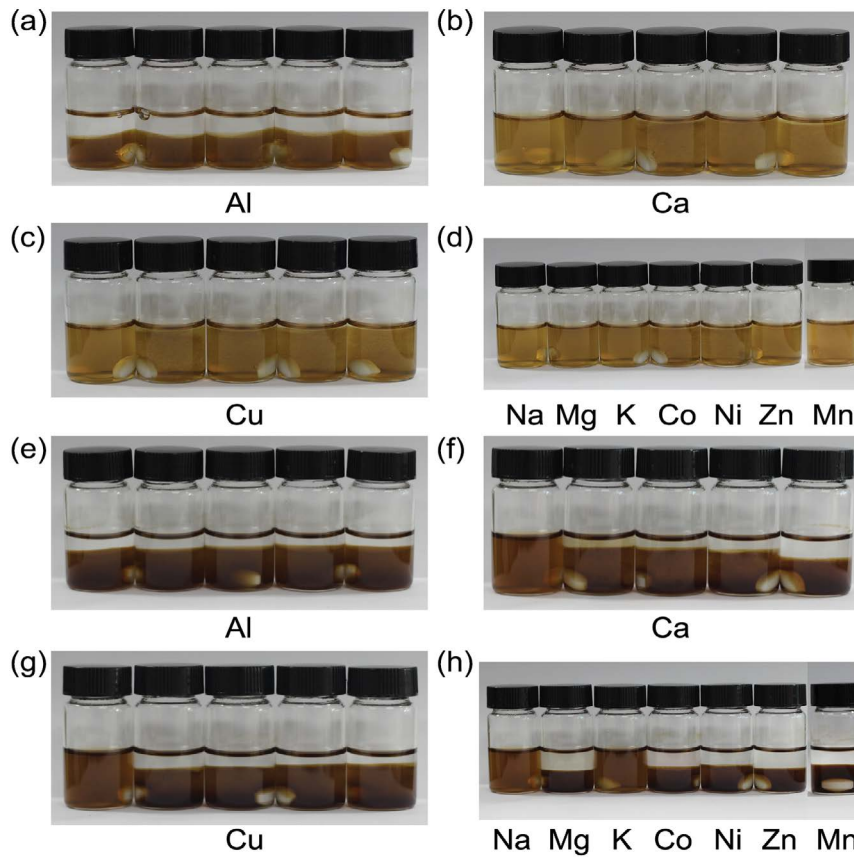


Fig. S5. Digital photographs were taken after the coagulation experiments with an initial GO concentration of (a–d) 200 mg/L and (e–h) 400 mg/L. The initial concentration ratio with Al^{3+} , Ca^{2+} , Cu^{2+} added were 0.4, 0.8, 1.2, 1.6 and 2.0 from left to right, and the initial concentration ratio with other cations added was fixed at 2.0.

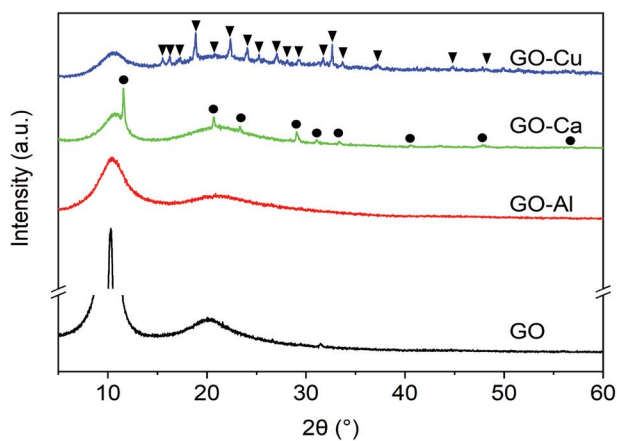


Fig. S6. XRD patterns of GO, GO-Al, GO-Ca and GO-Cu. The circle and triangle represent the XRD peaks of $\text{CaSO}_4 \cdot 2\text{H}_2\text{O}$ and $\text{CuSO}_4 \cdot 5\text{H}_2\text{O}$, respectively.

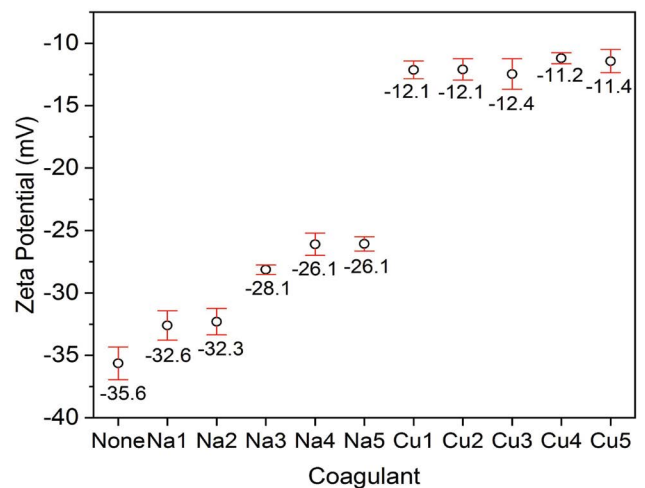


Fig. S7. Zeta potential of GO suspension with different coagulants added. $C_{\text{GO}} = 100$ mg/L. The concentration of Na_2SO_4 (Na1 to Na5) or CuSO_4 (Cu1 to Cu5) ranged from 40 to 200 mg/L.

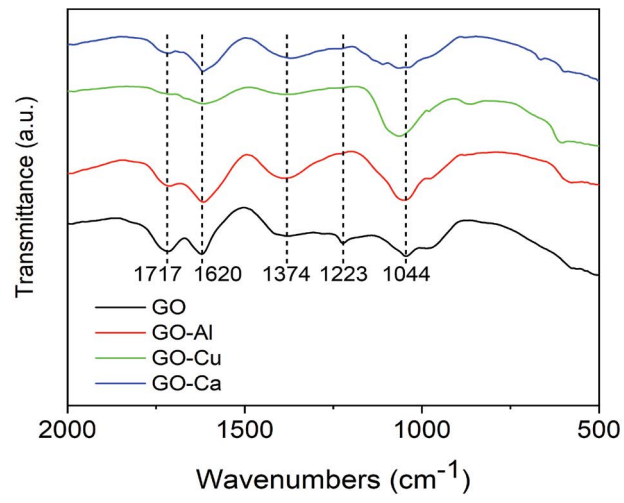


Fig. S8. FTIR spectra of GO, GO-Al, GO-Ca and GO-Cu.